Low-temperature sequence of phase transitions in $LiKSO_4$ studied by EPR

G. J. Perpétuo, M. S. S. Dantas, R. Gazzinelli, and M. A. Pimenta
Departamento de Fisica, Universidade Federal de Minas Gerais, Caixa Postal 702, 30161 Belo Horizonte, Brazil

(Received 31 May 1991; revised manuscript received 17 October 1991)

The low-temperature sequence of phase transitions in $LiKSO_4$ has been studied by EPR using the paramagnetic center Tl^{2+}. The coexistence of different phases in some temperature ranges is demonstrated. An axial-symmetry phase has been observed at 77 K after a fast cooling process. The ferroelastic phase (below 190 K) has been studied by applying uniaxial pressure. The existence of twinnings within each ferroelastic domain and a monoclinic-symmetry structure for this phase are found. A tilting of the paramagnetic tensors has been observed below 190 K, reflecting the freezing of the sulfate-ion orientational disorder. A model for the ferroelastic structure is proposed.

I. INTRODUCTION

In recent years a number of compounds of the family $A'A''BX_4$ [where A', A''=Li, Na, K, Rb, Cs, NH_4, $N(CH_3)_4$, etc., and BX_4=SO_4, SeO_4, $ZnCl_4$, $ZnBr_4$, BeF_4, MoO_4, WO_4, etc.] have been the object of great interest because of the variety of physical properties found in its sequence of phase transitions, including, for example, incommensurate, superionic, ferroelectric, and ferroelastic phases.[1] With the exception of superionic conductors (Li_2SO_4, $LiNaSO_4$, etc), the $A'A''BX_4$ compounds share a high-temperature disordered phase, belonging to the hexagonal space group D^4_{6h}.

Kurzynski[2] has recently classified these compounds in four distinct groups according to their sequence of structural phases. Lithium potassium sulfate ($LiKSO_4$) has been considered an individual case because of its unusual sequence of phase transitions, which is summarized below:

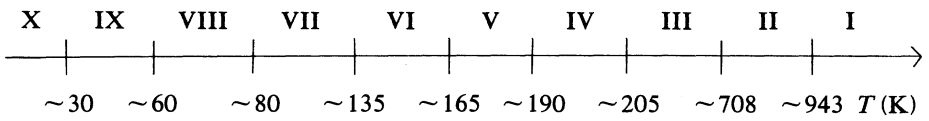

The temperatures in this scheme correspond to an average of the values found in the literature on the cooling process.[3-9]

In spite of the great number of experimental and theoretical works devoted to lithium potassium sulfate in the temperature range 20–1000 K, there are still a number of controversial points in its sequence of phase transitions. These controversies are basically related to the existence, or lack thereof, of some of these phase transitions and to the symmetry of some structural phases.

In fact, only the structures proposed for phases I and III are well established. The highest temperature phase (I) has a hexagonal symmetry belonging to the space group D^4_{6h} ($P6_3/mmc$).[10] The room-temperature phase (III) has also a hexagonal symmetry belonging to the space group C^6_6 ($P6_3$) with two formula units per unit cell.[11,12] Between these hexagonal phases there is a structural phase (II) with symmetry certainly lower than hexagonal. For this phase two structures have been proposed: an orthorhombic structure[13] and a modulated structure. The modulated structure is incommensurate between 743 and 940 K, and commensurate in the temperature range 711–743 K.[10] Recently, Pimenta *et al.*[14] proposed a model that reconciles these two explanations: a double-**k** orthorhombic modulation of the disorder probability.

Figure 1 shows the projection of the room-temperature structure in a plane normal to the hexagonal c axis.[11,12] The potassium ions are localized along the hexagonal axis (Wyckoff position a). The sulfate ions are oriented such that three oxygen ions [denoted as O(2)] form a plane perpendicular to the hexagonal axis and the fourth one [denoted as O(1)] is localized along the ternary axis of this structure (Wyckoff position b). The lithium and sulphur ions are also localized along the ternary axis. The two sulfate ions of the same unit cell are related by a sixfold screw axis along the c axis. Because of the polar character of its symmetry group, the crystal is pyroelectric at room temperature.[15] It presents also optical activity along the hexagonal axis in this phase.[9,15] Another important aspect of the room-temperature structure of $LiKSO_4$ is related to the dynamic orientational disorder of the sulfate ions. Schulz, Zucker, and Frech[12] have observed that the oxygen ion O(1) occupies in fact three different positions around the ternary axis. The average position is along the ternary axis, and this preserves the

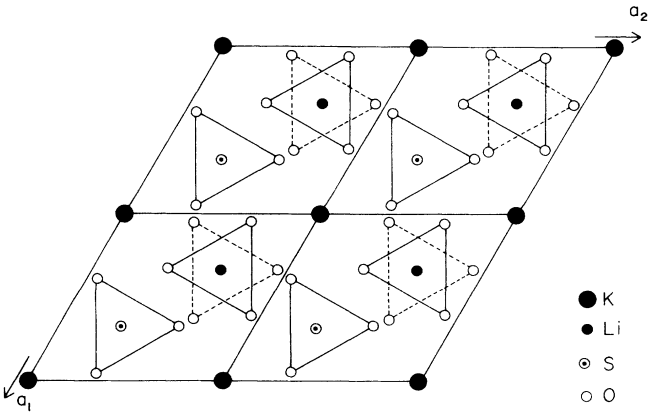

FIG. 1. Projection of four unit cells of $LiKSO_4$ in the basal plane for phases III and IV. The solid triangles represent the orientation of the sulfate tetrahedra in phase III. One sulfate in each unit cell is reorientated in phase IV (dashed triangles). The two tetrahedra in a unit cell are displaced by $c/2$ along the c axis.

hexagonal symmetry of the structure.

With decreasing temperature the crystal undergoes another phase transition around 205 K. Bansal *et al.*,[3] based on their Raman study, proposed a trigonal structure for phase IV belonging to the space group C_{3v}^4 ($P31c$). Tomaszewski and Lukaszewicz[4] have suggested, on the other hand, a C_{6v}^4 ($P6_3mc$) hexagonal structure. In a recent neutron-diffraction study, Zhang, Yan, and Boucherle[16] supported the trigonal symmetry proposed initially by Bansal *et al.*[3] and determined the atomic positions in this structure. Bhakay-Tamhane and Sequeira[7] have suggested that the presence of twins of small size could lead Tomaszewski and Lukaszewicz[4] to propose a higher-symmetry structure.

The projection of the trigonal structure in the basal plane is also showed in Fig. 1. The only difference in this structure with respect to the room-temperature structure is a rotation of one sulfate in each unit cell. Zhang, Yan, and Boucherle[16] showed that disorder in the orientation of the sulfate ions persists in this phase.

Continuing the cooling process, the crystal undergoes another phase transition around 190 K. Once again, there are some controversies with respect to the crystalline structure below this phase transition. A monoclinic structure[7,9] has been proposed belonging to the space group C_s^4 (Cc) and an orthorhombic structure[6] belonging to the space group C_{2v}^{12} ($Cmc2_1$). Kleemann, Schäfer, and Chaves[9] have observed a complicated domain superposition below 190 K in their crystal optical study. Another important feature of the IV-V phase transition is the freezing of the orientational disorder, resulting in a tilting of the sulfate tetrahedra.[4,7] Further, Breczewski, Krajewski, and Mróz[17] have observed the presence of ferroelastic domains in this phase.

Very little is known about the structure of the lower-temperature phases. Some authors have reported the existence of a phase transition around 165 K,[4,7] but there is no consensus in the literature. There is another controversy related to the crystaline structure at 80 K. A low-symmetry structure at that temperature has been proposed.[7,9] Some EPR studies revealed, on the other hand, a structure of axial symmetry.[5,18] Fonseca *et al.*[5] have proposed a reentrant hexagonal structure of phase VII.

A last important point concerns the kinetics of the sequence of low-temperature phase transitions in $LiKSO_4$. It has been emphasized by Tomaszewski and Lukaszewicz[4] that this sequence is strongly influenced by the thermal cycle employed and by the presence of defects and twinnings in the samples. Bhakay-Tamhane and Sequeira[7] have also observed a coexistence of different structures in some temperature ranges around the phase transitions.

In order to clarify some of these controversial points in the sequence of low-temperature phase transitions of $LiKSO_4$, we have studied this crystal by EPR using the center Tl^{2+} as paramagnetic probe. A complete analysis of the symmetry of the EPR spectra is presented here for phases III, IV, and V.

II. EXPERIMENTAL DETAILS AND THE SPIN HAMILTONIAN

The crystals have been grown by Dr. G. M. Ribeiro, from the slow evaporation of a saturated aqueous solution containing equimolar proportions of K_2SO_4 and Li_2SO_4 as well as 1 mol% of Tl_2SO_4. The sample presents an hexagonal prism morphology which permits an immediate identification of the hexagonal axis (c axis). The a axis has been identified by x-ray diffraction as being perpendicular to the c axis and parallel to a natural face of the crystal.

The EPR spectra have been recorded in an X-band spectrometer adapted to work with a uniaxial-pressure system. The temperature has been controlled within 0.5 K. The paramagnetic centers Tl^{2+} have been created by x-ray irradiation at 77 K and occupy the sites of the potassium ions. This paramagnetic enter has been chosen because of two major advantages: (i) its electronic spin $S=\frac{1}{2}$ does not permit fine structure and (ii) the existence of a strong hyperfine interaction with nuclear spin ($I=\frac{1}{2}$) which increases the resonant magnetic-field values, preventing superpositions due to other paramagnetic centers created by x-ray irradiation (as, for example, SO_4^-). The EPR spectra have been analyzed by using the spin Hamiltonian given by

$$\mathcal{H}=\mu_B \mathbf{H}\cdot\mathbf{g}\cdot\mathbf{S}+\mathbf{S}\cdot\mathbf{A}\cdot\mathbf{I}\ ,$$

where the first term represents the electronic Zeeman interaction ($\mathbf{H}$ is the static magnetic field and μ_B is the Bohr magneton) and the second one the hyperfine interaction between the electronic spin $\mathbf{S}$ and nuclear spin $\mathbf{I}$. The second-rank Zeeman ($\mathbf{g}$) and hyperfine ($\mathbf{A}$) tensors reflect the intensity and anisotropy of these interactions. Only two of the four permitted magnetic transitions are observed in an X-band EPR spectrometer and are localized at about 6000 and 7000 G, respectively. From now on we will call them low-field and high-field lines.

III. RESULTS AND DISCUSSION

Figure 2 shows the temperature dependence of the low-field EPR spectra for the static magnetic field parallel to the c axis. The cooling rate was about 1.5 K/min. At room temperature we can observe a single line in the low-field region. The slight asymmetric profile of this line is ascribed to the small difference in the magnetic moments of the isotopes ^{205}Tl and ^{203}Tl with a relative abundance of 70.5% and 29.5%, respectively. We can observe in Fig. 2 the appearance of a second line at about 225 K. The intensity of this line increases, while the first one decreases with decreasing temperature. This is clear evidence of the coexistence of phases III and IV in a temperature range around the phase transition, as already observed by some authors.[4,7] At about 183 K we can observe the appearance of a third line, revealing the beginning of the IV-V phase transition. Here, again, a coexistence of phases IV and V is observed around the phase transition. These results are summarized in Fig. 3, which shows the temperature dependence of the relative intensity of the EPR lines associated with phases III, IV, and V. On the heating process we have also observed a coexistence of phases at the V-IV and IV-III phase transitions. The temperatures of the beginning of these transitions were about 190 and 248 K, respectively, revealing an important thermal hysteresis for the III-IV phase transition.

We may note here that there is no group-subgroup relation between the symmetry of phases III and IV (C_6^6 and C_{3V}^4). The trigonal structure of phase IV has the same number of symmetry elements as the room-temperature hexagonal structure. If some symmetry elements are lost in the III-IV phase transition (three sixfold screw axes), some others appear below the phase transition (three vertical c glide planes). It means that this phase transition is reconstructive rather than a symmetry-breaking one (Landau type). This fact is clearly related to the slow kietics of this phase transition, which gives rise to an important thermal hysteresis (up to 50 K), and the coexistence of different structures over a large temperature range.

It may be observed that all these results are strongly affected by the thermal cycle employed. We have observed that, if the sample is cooled down to 77 K at a very fast rate, a spectrum revealing a structure with axial symmetry is found at low temperatures. By using a slow cooling rate, we have found absolutely different spectra, revealing a structure of low symmetry. We have concluded that, on a very fast cooling process, the room-temperature structure is frozen out at 77 K. This conclusion can explain the observation of a reentrant hexagonal phase by Fonseca *et al.*[5] and an axial structure at low temperature by Bill, Ravi Sekhar, and Lovy[18] in their EPR spectra. In both cases the paramagnetic centers

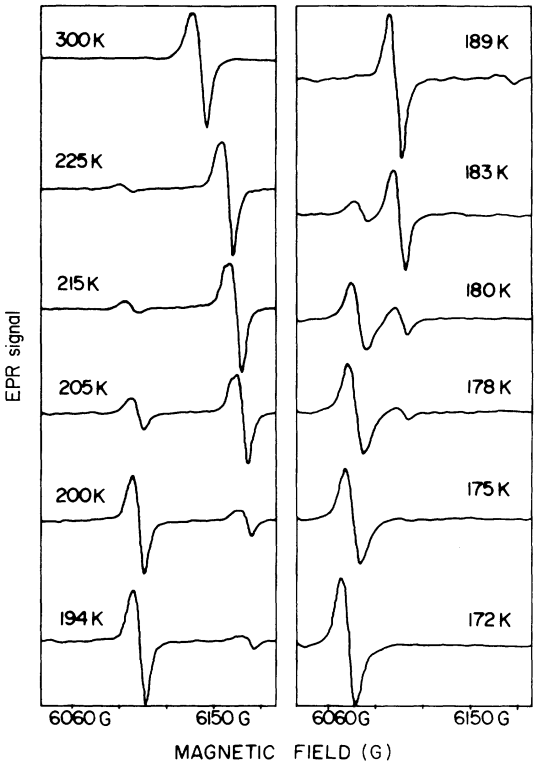

FIG. 2. Temperature dependence of the low-field EPR spectra of the center Tl^{2+} in $LiKSO_4$ for the static magnetic field parallel to the c axis.

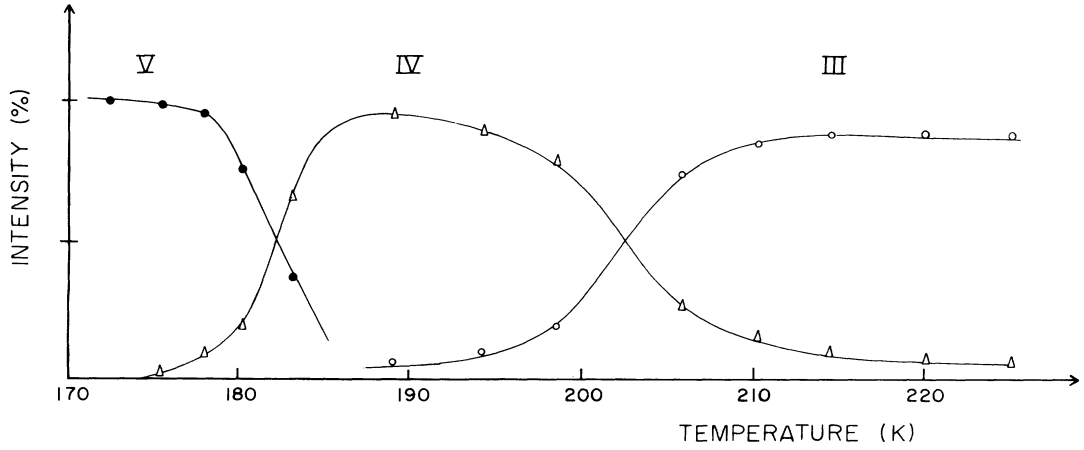

FIG. 3. Temperature dependence of the relative intensity of the EPR lines associated with phases III, IV, and V.

were created by x-ray irradiation at 77 K and the spectra have been obtained without heating the crystal. We have observed that this axial frozen structure remains stable for several days if one keeps the crystal at liquid-nitrogen temperature.

A. Angular dependence of the spectra of phases III and IV

We present here a simultaneous description of the results obtained for phases III and IV due to the similitude of the behavior of the angular dependence of their spectra. The angular dependences for these phases have been performed at 300 and 197 K, respectively. As can be observed in Fig. 4, there is only one line in the low-field region and another one in the high-field region for any orientation of the static magnetic field. It is also observed that the resonant field does not vary for the static magnetic field in any direction in the *ab* plane. We may conclude that the Zeeman and hyperfine tensors are axial (with the same principal values in the *ab* plane) and the *z* principal axis coincides with the *c* crystallographic axis. These results are compatible with the structures proposed for phases III and IV (C_6^6 and C_{3v}^4, respectively) since in both structures the potassium ions (and then the paramagnetic centers) occupy two different sites of point symmetry C_3 (Wyckoff position a) which are magnetically equivalent. An important point here is that the Tl^{2+} paramagnetic center does not break the axial symmetry of the potassium-ion site. The parameters of the magnetic tensors which have fitted the experimental angular dependence of the resonant fields in phases III and IV are shown in Table I.

B. Angular dependence of the spectra of phase V

The EPR spectra of this phase have been obtained at 172 K. Figure 5 shows the angular dependence of the resonance lines. Only one line is observed for the static magnetic field along the *c* axis (considering only the low-field region), while three lines are observed for the magnetic field along the *a* and *b* axes. For **H** in the crystallographic *ab*, *ac*, and *bc*, planes up to six lines can be observed. The analysis of the maxima and minima of the angular dependence of the resonance lines in the *ab* plane has led us to draw the projection of the magnetic tensors in this plane, represented by the six ellipses in Fig. 6. We can observe in this figure three pairs of ellipses, rotated with respect to each other by 120° around the *c* axis. This result reflects the existence of three ferroelastic domains observed by Breczewski, Krajewski, and Mróz.[17]

At the beginning of the experiment, we have chosen arbitrarily a system (*S*) of crystallographic axes to perform the angular dependence of the spectra. System *S* corresponds to one particular ferroelastic domain. We may introduce the systems *S'* and *S''* rotated in relation to *S* by $+120°$ and $-120°$, respectively, to describe the two other ferroelastic domains. In order to associate the correct pair of lines of Fig. 5 with each ferroelastic domain, we have performed some experiments by applying uniaxial pressure perpendicular to the *c* axis. Tomaszewski and Lukaszewicz[4] have proposed that the ferroelastic deformation corresponds to the elongation of the lattice parameter *a* and the shortening of the parameter *b*. By applying uniaxial pressure parallel to the *b* axis, the *S* ferroelastic domain will be favored since the two other domains have a component of elongation in this direction. Figure 7 shows the alteration of the EPR spectra ($\mathbf{H}\|a$) when uniaxial pressure is applied parallel to the *b* axis. We have observed the disappearance of two lines and an increase of the third one with increasing pressure.

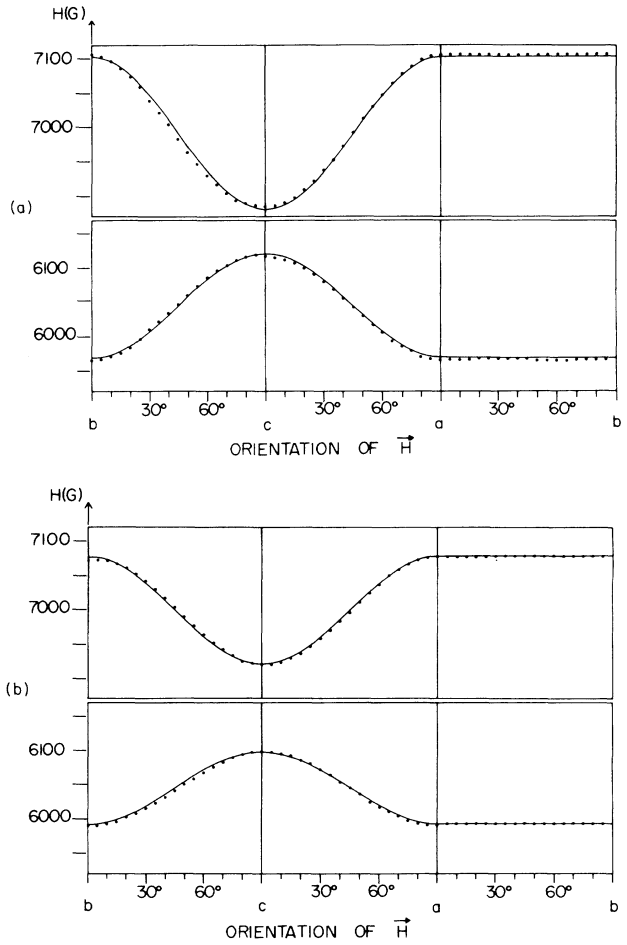

FIG. 4. Angular dependence of the EPR lines in the three crystallographic planes: (a) phase III and (b) phase IV. The solid lines represent the best fit of the experimental data.

TABLE I. Principal values (parallel and perpendicular) of the magnetic tensors for phases III and IV.

Phase	$g_\parallel$	$g_\perp$	$A_\parallel$ (MHz)	$A_\perp$ (MHz)
III	1.9980	1.9957	118 079	117 741
IV	2.0004	1.9984	119 684	119 447

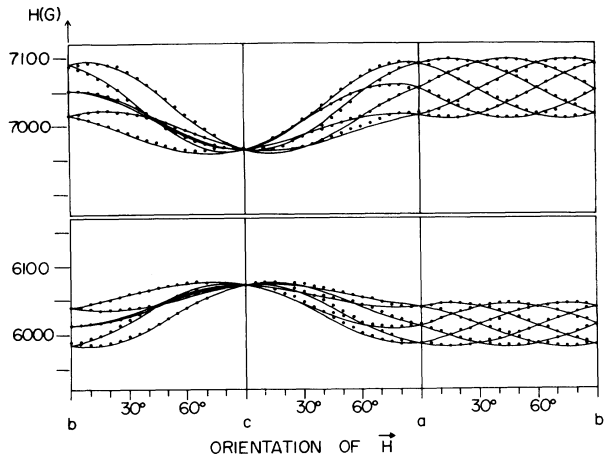

FIG. 5. Angular dependence of the EPR lines in the three crystallographic planes in phase V. The solid lines represent the best fit of the experimental data.

A ferroelastic monodomain has been induced with an uniaxial pressure of about 100 bars. This result has led us to assign each pair of resonance lines to the S, S', and S'' ferroelastic domains, as shown in Fig. 6. We can also observe that, within each domain, the two nonequivalent centers are related by a mirror plane σ_y.

C. Symmetry analysis of phase V

Let us compare now our experimental results with the two structural models proposed for this ferroelastic phase: a monoclinic (space group C_s^4) and an orthorhombic (space group C_{2v}^{12}) structure.

In the orthorhombic structure the paramagnetic center Tl^{2+} would occupy a site with symmetry σ_x (Wyckoff notation a). The magnetic tensors should be invariant under this symmetry operation; i.e., one of its principal axes should coincide with the a crystallographic axis. Figure 6 shows clearly that this is not the case. The projection of the principal axes in the ab plane are rotated by approximately 15° relative to the a axis. Our results would be compatible with an orthorhombic structure if the paramagnetic center had broken its site symmetry (a charge compensation in some preferential direction). However, it is difficult to support this hypothesis since the paramagnetic center has not broken the site symmetry in phases III and IV. In this sense an orthorhombic structure seems to be incompatible with our experimental results.

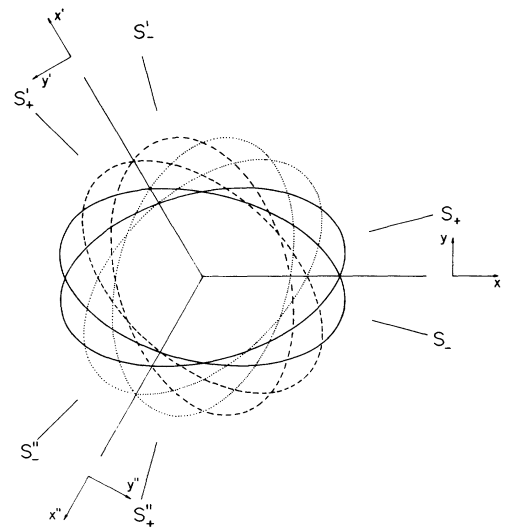

FIG. 6. Projection in the ab plane of the ellipsoids representing the magnetic tensors in phase V. The solid ellipses are associated with the S ferroelastic domain. The dashed and dotted curves are associated with the S' and S'' domains, respectively. The symmetry operations relating the pairs (S_+,S_-), (S'_+,S'_-), and (S''_+,S''_-) are carried out with respect to the S (x,y,z), S' $(x,',y',z')$, and S'' (x'',y'',z'') systems of axes, respectively.

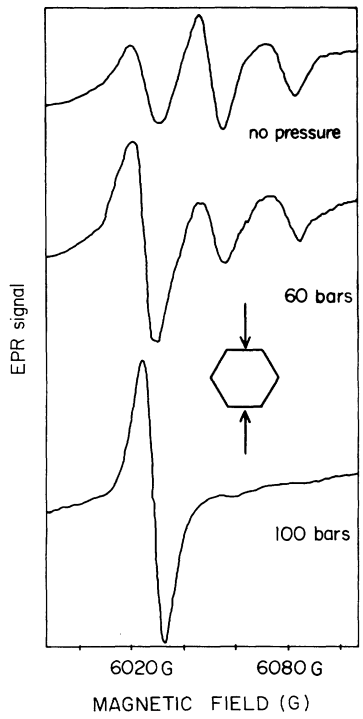

FIG. 7. Pressure dependence of the EPR spectra of phase V for $\mathbf{H}\|a$. The uniaxial pressure is applied along the b axis.

The two distinct sites for the paramagnetic center in one ferroelastic domain are related by a mirror plane σ_y, and then the projection of its magnetic tensors must coincide in the ac plane. Therefore, only three lines should be expected for $\mathbf{H}$ lying in this plane, corresponding to the pairs (S_-,S_+), (S'_-,S''_+), and (S''_-,S'_+). However, as shown in Fig. 5, six lines have been observed for $\mathbf{H}$ in this plane. Moreover, for $\mathbf{H}$ in a general orientation, clearly more than six lines have been observed in the spectra. To explain our results we must take into account the existence of twinnings in the sample and the symmetry operations relating them.

In the monoclinic structure the paramagnetic center occupies sites with symmetry C_1, which does not impose restrictions on the elements of the magnetic tensors. As there are two distinct sites for the paramagnetic center (denoted by $+$ and $-$) and three ferroelectric domains (denoted by S, S', and S''), six lines are expected for the general direction of the external magnetic field $\mathbf{H}$.

TABLE II. First row of the table gives the elements of symmetry of the C_6 hexagonal group, considering a particular twin domain denoted by A. The three other rows of the table are generated considering the three types of twin domains (denoted by B, C, and D) related to this first one by the symmetry operations σ_z, σ_y, and C_{2x}.

Twin	Elements of symmetry					
A	E	C_6	C_3	C_{2z}	C_3^{-1}	C_6^{-1}
B	σ_z	S_6	S_3	i	S_3^{-1}	S_6^{-1}
C	σ_y	$\sigma_{x'}$	$\sigma_{y''}$	σ_x	$\sigma_{y'}$	$\sigma_{x''}$
D	C_{2x}	$C_{2y'}$	$C_{2x''}$	C_{2y}	$C_{2x'}$	$C_{2y''}$

TABLE III. First row of the table gives the elements of symmetry of the C_{3v} trigonal group, considering a particular twin domain denoted by A. The three other rows of the table are generated considering the three types of twin domains (denoted by B, C, and D) related to this first one by the symmetry operations σ_z, σ_x, and C_{2y}.

Twin	Elements of symmetry					
A	E	C_3	C_3^{-1}	σ_y	$\sigma_{y''}$	$\sigma_{y'}$
B	σ_z	S_3	S_3^{-1}	C_{2x}	$C_{2x''}$	$C_{2x'}$
C	σ_x	$\sigma_{x''}$	$\sigma_{x'}$	C_{2z}	C_6^{-1}	C_6
D	C_{2y}	$C_{2y''}$	$C_{2y'}$	i	S_6^{-1}	S_6

TABLE IV. Twenty-four elements of symmetry relating the possible potassium-ion sites in the structure of phase V, considering the two elements of the monoclinic group C_s, the four types of twins (A, B, C, and D), and the three ferroelastic domains S, S', and S''.

Twin	S		S'		S''	
A	E	σ_y	C_3	$\sigma_{y'}$	C_3^{-1}	$\sigma_{y''}$
B	σ_z	C_{2x}	S_3	$C_{2x'}$	S_3^{-1}	$C_{2x''}$
C	σ_x	C_{2z}	$\sigma_{x''}$	C_6	$\sigma_{x'}$	C_6^{-1}
D	C_{2y}	i	$C_{2y''}$	S_6	$C_{2y'}$	S_6^{-1}

TABLE V. Principal values of the Zeeman and hyperfine tensors and its orientation relative to the crystallographic axes for a particular domain of phase V.

	Principal values		Orientation		
	g	A (MHz)	a	b	c
x	1.9991	120 180	19°	107°	83°
y	1.9991	120 313	72°	25°	106°
z	2.0004	120 394	92°	73°	17°

D. Considerations about twinnings in the sample

Let us return to the hexagonal structure of room temperature (C_6^6). Klapper, Hahn, and Chung[15] have observed the existence of four types of twin domains at room temperature, related to the four possibilities of combinations of polarity (up and down) and optical activity (right and left handed). They observed that these twin domains are related to each other by symmetry elements of phase I ($T > 943$ K) which are not present in the room-temperature structure (phase III), i.e., σ_y $(x,y,z \rightarrow x,\bar{y},z)$, σ_z $(x,y,z \rightarrow x,y,\bar{z})$, and C_{2x} $(x,y,z \rightarrow x,\bar{y},\bar{z})$. Let us now analyze the effect of applying these symmetry operations on the six elements of the point group C_6. Starting from a particular twin domain (denoted by A), whose elements of symmetry are given in the first row of Table II, and considering the three other types (denoted by B, C, and D) related to this first one by the symmetry operations σ_z, σ_y, and C_{2x}, we can construct the three other rows of Table II using the following relations: $B=\sigma_z A$, $C=\sigma_y A$, and $D=C_{2x} A$. It is interesting to note that all 24 elements of the symmetry of the highest-temperature phase (D_{6h}) are present in this table.

The III-IV phase transition is accompanied by a rotation of one sulfate ion in each unit cell, as shown in Fig. 1. Two equivalent structures can be generated below the transition temperature, since there are two sulfate ions in a unit cell. These two twinned structures are related by a symmetry operation σ_x. Considering this effect in the four twin domains of phase III, we arrive again at four types of twins in phase IV (there is a coincidence by pairs), which are related by the following relations: $B=\sigma_z A$, $C=\sigma_x A$, and $D=C_{2y} A$. Taking them into account, we arrive at Table III in which all 24 elements of the highest-temperature phase are also present, but arranged in a different manner in relation to that of the room-temperature structure.

The decrease of symmetry in the IV-V phase transition gives rise to three types of ferroelastic domains which are related between each other by the symmetry operations C_3 and C_3^{-1} which have been lost with respect to phase IV. Then the six elements of the first line of Table III can be grouped, forming the three pairs of elements corresponding to the three ferroelastic domains. Considering the twin laws σ_z, σ_x, and C_{2y}, we generate the 12 possible structures for this phase (Table IV).

We must remember that the magnetic tensors of phases III and IV are axial and its principal axes coincide with the crystallographic ones. Then the paramagnetic centers of the twinned structures are magnetically equivalent, giving rise to only one resonance line in these phases. In the ferroelastic phase the magnetic tensors are no longer axial and its principal axes are no longer parallel to the crystallographic ones. In this case the EPR spectra must reflect the existence of twinnings in the sample, and then we shall introduce in our analysis the elements of symmetry given in Table IV. Only 12 magnetically nonequivalent centers are expected since the spin Hamiltonian is invariant under the inversion-symmetry operation. We have observed, in fact, up to 12 lines for the general direction of the static magnetic field **H** with respect to the crystallographic axes.

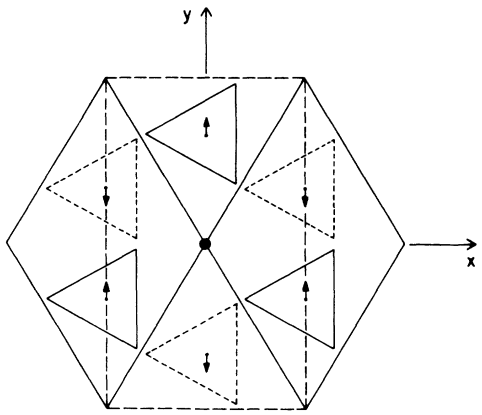

FIG. 8. Projection in the basal plane for the proposed structure of phase V. The central point represents a possible site for the paramagnetic center. The arrows indicate oxygen-ion O(1) displacements, related to the tilts of the sulfate tetrahedra, yielding a monoclinic symmetry. The solid and dashed triangles represent sulfate tetrahedra displaced by $c/2$ along the c axis.

We have fitted the whole angular dependence of the resonance lines shown in Fig. 5, first by determining the components of the magnetic tensors for one paramagnetic center and then by introducing the symmetry operations presented in Table IV. The principal values of the Zeeman and hyperfine tensors as well as the orientation of the principal axes of one paramagnetic center are presented in Table V. We may observe that, in this phase, the magnetic tensors have three distinct principal values and its principal axes do not coincide with the crystallographic ones. It is also interesting to note that the z axis of the magnetic tensors is rotated 17° around an axis, practically parallel to a.

Tomaszewski and Lukaszewicz[4] have proposed that the IV-V phase transition is accompanied by a freezing of the sulfate ions in one of the three disordered directions of the structure of phase IV. Bhakay-Tamhane and Sequeira[7] suggested that the sulfate ions are tilted approximately 10° from the c direction. Our results give experimental support to this model. The inclination of the z axis of the magnetic tensors reflects the tilt of the sulfate ions below the phase transition. In this sense the freezing of the sulfate-ion orientational disorder may correspond to tilts of the tetrahedra around the a axis. The two sulfate ions of the trigonal unit cell turn in opposite senses since they are related by a c glide plane orthogonal to the b axis. A picture of the proposed structure for phase V is shown in Fig. 8. The arrows in this figure correspond to the direction of displacement of the oxygen ions O(1).

IV. CONCLUSIONS

As already emphasized in the Introduction, the two major problems in the sequence of low-temperature phase transitions in $LiKSO_4$ are related to the existence of some phase transitions and the symmetry of the low-temperature phases. With respect to the first point, it

seems clear now that the difficulty of determining the transition temperatures is related basically to the coexistence of different structures in some temperature ranges.[4,5,7,9] We have observed the coexistence of III-IV and IV-V structures over broad temperature ranges. The proposed V-VI phase transition at about 165 K has not been observed in our spectra. The complete disappearance of phase IV occurs approximately at that temperature.

Our results give some insight into the controversies concerning symmetry. First, we have observed absolutely different spectra at 77 K, depending on the cooling rate. An axial-symmetry structure has been observed at 77 K only after a very fast cooling process. This result suggests an aleatory freezing of sulfate-ion orientational disorder of room temperature, yielding an average hexagonal structure. It can explain the reentrant phase proposed by some authors.[5,18]

We have also demonstrated the importance of considering the existence of twin domains and the symmetry laws relating them. We have observed that, macroscopically, the crystal has an apparent symmetry greater than its real symmetry. It can explain the hexagonal and orthorhombic symmetries proposed by Tomaszewski and Lukaszewicz[4] for phases IV and V, respectively.

The axial symmetry of phases III and IV has been verified from the determination of the Zeeman and hyperfine tensors of the Tl^{2+} paramagnetic center. It has been possible to induce a ferroelastic monodomain in our sample below 190 K by applying uniaxial pressure. The angular dependence of the EPR spectra in the ferroelastic phase (V) revealed a monoclinic structure (probably belonging to the space group C_s^4) originating from the freeze out of the sulfate-ion orientational disorder. The inclination of the magnetic tensors gives experimental support to the freeze-out model and shows that the tilting of the SO_4 groups takes place around the a axis.

ACKNOWLEDGMENTS

We wish to thank Dr. G. M. Ribeiro for kindly providing us with the samples. We are also grateful to Dr. N. L. Speziali and Dr. J. F. Sampaio for helpful discussions, Dr. R. A. Nogueira for computational assistance, and C. J. Franco for providing access to the uniaxial-pressure system.

[1]H. Z. Cummins, Phys. Rep. **185**, 211 (1990).
[2]M. Kurzynski (unpublished).
[3]M. L. Bansal, S. K. Deb, A. P. Roy, and V. C. Sahni, Solid State Commun. **36**, 1047 (1980).
[4]P. E. Tomaszewski and K. Lukaszewicz, Phase Transit. **4**, 37 (1983).
[5]C. H. A. Fonseca, G. M. Ribeiro, R. Gazzinelli, and A. S. Chaves, Solid State Commun. **46**, 221 (1983).
[6]R. Cach, P. E. Tomaszewski, and J. Bornarel, J. Phys. C **18**, 915 (1985).
[7]S. Bhakay-Tamhane and A. Sequeira, Ferroelectrics **69**, 241 (1986).
[8]J. Mendes Filho, J. E. Moreira, F. E. A. Melo, F. A. Germano, and A. S. B. Sombra, Solid State Commun. **60**, 189 (1986).
[9]W. Kleeman, F. G. Schäfer, and A. S. Chaves, Solid State Commun. **64**, 1001 (1987).
[10]Y. Y. Li, Solid State Commun. **51**, 355 (1984).
[11]A. J. Bradley, Philos. Mag. **49**, 1225 (1925).
[12]H. Schulz, U. Zucker and R. Frech, Acta Crystallogr. B **41**, 21 (1985).
[13]S. J. Chung and T. Hahn, Acta Crystallogr. A **28**, 557 (1972).
[14]M. A. Pimenta, P. Echegut, Y. Luspin, G. Hauret, F. Gervais, and P. Abelard, Phys. Rev. B **39**, 3361 (1989).
[15]H. Klapper, T. Hahn, and S. J. Chung, Acta Crystallogr. B **43**, 147 (1987).
[16]P. L. Zhang, Q. W. Yan, and J. X. Boucherle, Acta Crystallogr. C **44**, 592 (1988).
[17]T. Breczewski, T. Krajewski, and B. Mróz, Ferroelectrics **33**, 9 (1981).
[18]H. Bill, Y. Ravi Sekhar, and D. Lovy, J. Phys. C **21**, 2795 (1988).